

Better-Than-Chance Classification for Signal Detection

Jonathan Rosenblatt Roei Gilron Roy Mukamel

August 16, 2016

Abstract

[TODO]

1 Introduction

A common workflow in neuroimaging consists of fitting a classifier, and estimating its predictive accuracy using cross validation. Given that the cross validated accuracy is a random quantity, it is then common to test if the cross validated accuracy is significantly better than chance using a permutation test. Examples in the neuroscientific literature include Golland and Fischl [2003], Pereira et al. [2009], Varoquaux et al. [2016], and especially the recently popularized *multivariate pattern analysis* (MVPA) framework of Kriegeskorte et al. [2006]. This practice is also observed in very high profile publications in the genetics literature: Golub et al. [1999], Slonim et al. [2000], Radmacher et al. [2002], Mukherjee et al. [2003], Juan and Iba [2004], Jiang et al. [2008].

To fix ideas, we will adhere to a concrete example. In Gilron et al. [2016], the authors seek to detect brain regions which encode differences between vocal and non-vocal stimuli. Following the MVPA workflow, the localization problem is cast as a supervised learning problem: if the type of the stimulus can be predicted from the spatial activation pattern significantly better than chance, then a region is declared to encode vocal/non-vocal information. We call this an *accuracy test*, a.k.a. *class prediction*, or *pattern discrimination*.

This same signal detection task can be also approached as a two-group multivariate test. Inferring that a region encodes vocal/non-vocal information, is essentially inferring that the spatial distribution of brain activations is different given a vocal/non-vocal stimulus. As put in Pereira et al. [2009]:

... the problem of deciding whether the classifier learned to discriminate the classes can be subsumed into the more general question as to whether there is evidence that the underlying distributions of each class are equal or not.

A practitioner may then call upon a two-group population test such as Hotelling’s T^2 [Anderson, 2003]. Alternatively, if the size of a brain region is large compared to the number of observations, so that the spatial covariance cannot be fully estimated, then a high dimensional version of Hotelling’s test can be called upon, such as in Schäfer and Strimmer [2005] or Srivastava [2007]. For brevity, and in contrast to *accuracy tests*, we will call any two-sample multivariate tests simply *population tests*, also termed *class comparisons*. [TODO: rename to parameter test?]

At this point, it becomes unclear which is preferable: a population test or an accuracy test? The former with a heritage dating back to Hotelling [1931], and the latter being extremely popular, as the 959 citations¹ of Kriegeskorte et al. [2006] suggest.

The comparison between population and accuracy tests was precisely the goal of Ramdas et al. [2016], who compared the T^2 population test to the accuracy of *Fisher’s linear discriminant analysis* classifier (LDA). By comparing the rates of convergence of the powers to 1, Ramdas et al. [2016] concluded that accuracy and population tests are rate equivalent.

Asymptotic relative efficiency measures (ARE) are typically used by statisticians to compare between rate-equivalent test statistics [van der Vaart, 1998]. Ramdas et al. [2016] derive the asymptotic power functions of the two test statistics, which allows to compute the ARE between Hotelling’s T^2 (population) test and Fisher’s LDA (accuracy) test. Theorem 14.7 of van der Vaart [1998] relates asymptotic power functions to ARE. Using the results of Ramdas et al. [2016] we deduce that the ARE is lower bounded by $2\pi \approx 6.3$. This means that Fisher’s LDA requires at least 6.3 more samples to achieve the same (asymptotic) power than the T^2 test. In this light, the accuracy test is remarkably inefficient compared to the population test. For comparison, the t-test is only 1.04 more (asymptotically) efficient than Wilcoxon’s rank-sum test [Lehmann, 2009], so that an ARE of 6.3 is strong evidence in favor of the population test.

Before discarding accuracy tests as inefficient, we recall that Ramdas et al. [2016] analyzed a *half-sample* holdout. The authors conjectured that a leave-one-out approach, which makes more efficient use of the data, may have better performance. Also, the analysis in Ramdas et al. [2016] is asymptotic. This eschews the discrete nature of the accuracy statistic, which will be

¹GoogleScholar. Accessed on Aug 4, 2016.

65 shown to have crucial impact. Since typical sample sizes in neuroscience are
66 not large, we seek to study which test is to be preferred in finite samples?
67 Our conclusion will be quite simple: *population tests almost always have more*
68 *power than accuracy tests.*

69 Our statement rests upon the observation that with typical sample sizes,
70 the accuracy test statistic is highly discrete. Permutation testing with dis-
71 crete test statistics are known to be conservative [Hemerik and Goeman,
72 2014], since they are insensitive to mild perturbations of the data, and they
73 cannot exhaust the permissible false positive rate. The degree of discretiza-
74 tion is governed by the number of samples. In our neuroscience example
75 from Gilron et al. [2016], the classification is performed based on 40 trials,
76 so that the test statistic may assume only 40 possible values. This number
77 of examples is not unusual if considering this is the number of trial-repeats,
78 or the number of subjects in an neuroimaging study.

79 The discretization effect is aggravated if the test statistic is highly concen-
80 trated. For an intuition consider the usage of a the *resubstitution accuracy*
81 as a test statistic. This statistic simply means that the accuracy is not cross
82 validated. If the data is high dimensional, the resubstitution accuracy will be
83 very high due to over fitting. In a very high dimensional model, the resubsti-
84 tution accuracy will be 1 for the observed data [McLachlan, 1976, Theorem
85 1], but also for any permutation. The concentration of resubstitution accu-
86 racy near 1, and its discreteness, render this test completely useless, with a
87 power tending to 0 for any (fixed) effect size, as the dimension of the model
88 grows.

89 To compare the power of accuracy tests and population tests in finite sam-
90 ples, we perform a simulation study of a battery of test statistics. We start
91 with formalizing the problem in Section 2. The main findings are reported
92 in Sections 4 and 5. A discussion follows in Section 6.

93 2 Problem setup

94 Let $y \in \mathcal{Y}$ be a class encoding. Let $x \in \mathcal{X}$ be a p dimensional feature vector.
95 In our vocal/non-vocal example we have $\mathcal{Y} = \{-1, 1\}$ and p , the number of
96 voxels in a brain region so that $\mathcal{X} = \mathbb{R}^{27}$.

97 Given n pairs of (x_i, y_i) , typically assumed i.i.d., a population test amounts
98 to testing whether $x|y = 1$ has the the same distribution as $x|y = -1$. I.e.,
99 we test if the multivariate voxel activation pattern has the same distribution
100 when given a vocal stimulus, as when given a non-vocal stimulus.

An accuracy test amounts to learning a predictive model and testing if its
predictions $y|x$ are better than chance. Denoting a dataset by $\mathcal{S} := (x_i, y_i)_{i=1}^n$,

the a predictor, $\mathcal{A}_{\mathcal{S}}(x) : \mathcal{X} \rightarrow \mathcal{Y}$, is the output of a learning algorithm \mathcal{A} when applied to the dataset, $\mathcal{A} : \mathcal{S} \rightarrow \mathcal{A}_{\mathcal{S}}(x)$. The accuracy of predictor $\mathcal{A}_{\mathcal{S}}(x)$ is defined as the probability of $\mathcal{A}_{\mathcal{S}}(x)$ making a correct prediction. Denoting by \mathcal{P} the probability measure of (x, y) , and by \mathcal{P}^n the same for the i.i.d sample \mathcal{S} , then

$$\mathcal{E}_{\mathcal{A}_{\mathcal{S}}(x)} := \mathcal{P}(\mathcal{A}_{\mathcal{S}}(x) = y). \quad (1)$$

The accuracy of an algorithm \mathcal{A} is defined as the average accuracy, over all possible data sets

$$\mathcal{E}_{\mathcal{A}} := \int_{\mathcal{S}} \mathcal{E}_{\mathcal{A}_{\mathcal{S}}} d\mathcal{P}^n(\mathcal{S}). \quad (2)$$

101 Denoting an estimate of $\mathcal{E}_{\mathcal{A}_{\mathcal{S}}(x)}$ by $\hat{\mathcal{E}}_{\mathcal{A}_{\mathcal{S}}(x)}$, and $\mathcal{E}_{\mathcal{A}}$ by $\hat{\mathcal{E}}_{\mathcal{A}}$, a statistically sig-
 102 nificant “better than chance” estimate of either, is evidence that the classes
 103 are distinct. In a typical application, the predictor is not fixed, so that $\hat{\mathcal{E}}_{\mathcal{A}}$,
 104 and not $\hat{\mathcal{E}}_{\mathcal{A}_{\mathcal{S}}(x)}$, will be used for the testing.

105 Two popular estimates of $\hat{\mathcal{E}}_{\mathcal{A}}$ are the *resubstitution estimate*, and the
 106 V-fold cross validation (CV) estimate [Hastie et al., 2003].

Definition 1 (Resubstitution accuracy). The resubstitution accuracy estimator, $\hat{\mathcal{E}}_{\mathcal{A}}^{resub}$, is defined as

$$\hat{\mathcal{E}}_{\mathcal{A}}^{Resub} := \frac{1}{n} \sum_{i=1}^n \mathcal{I}\{\mathcal{A}_{\mathcal{S}}(x_i) = y_i\}, \quad (3)$$

107 where $\mathcal{I}\{A\}$ is the indicator function of event A .

Definition 2 (V-fold CV). Denoting by \mathcal{S}^v the v 'th partition of the dataset, and by $\mathcal{S}^{(v)}$ its complement, so that $\mathcal{S}^v \cup \mathcal{S}^{(v)} = \cup_{v=1}^V \mathcal{S}^v = \mathcal{S}$, the V-fold CV accuracy estimator, $\hat{\mathcal{E}}_{\mathcal{A}}^{Vfold}$, is defined as

$$\hat{\mathcal{E}}_{\mathcal{A}}^{Vfold} := \frac{1}{V} \sum_{v=1}^V \frac{1}{|\mathcal{S}^v|} \sum_{i \in \mathcal{S}^v} \mathcal{I}\{\mathcal{A}_{\mathcal{S}^{(v)}}(x_i) = y_i\}, \quad (4)$$

108 2.1 Candidate Tests

109 The design of a permutation test using $\hat{\mathcal{E}}_{\mathcal{A}}$, requires the following design
 110 choices:

- 111 1. Is $\hat{\mathcal{E}}_{\mathcal{A}}$ cross validated or not?

112 2. For a V-fold cross validated test statistic:

113 (a) Should the data be refolded in each permutation?

114 (b) Should the data folding be balanced (a.k.a. stratified)?

115 (c) How many folds?

116 3. How to estimate $\hat{\mathcal{E}}_{\mathcal{A}}$?

117 We will now address these questions while bearing in mind that unlike
118 the typical supervised learning setup, we are not interested in an unbiased
119 estimate of $\mathcal{E}_{\mathcal{A}}$, but rather in its mere departure from chance level.

120 **Cross validate or not?** Given our goal, a biased estimate of $\hat{\mathcal{E}}_{\mathcal{A}}$ is not a
121 problem provided that bias is consistent over all permutations. The under-
122 lying intuition is that a permutation test will be unbiased, provided that the
123 exact same computation is performed over all permutations. We will thus
124 be considering both cross validated accuracies, and *resubstitution accuracies*,
125 where the accuracy is evaluated on the training set and not on a holdout.

126 **Balanced folding?** The standard practice when cross validating is to con-
127 strain the data folds to be balanced, i.e. stratified [e.g. Ojala and Garriga,
128 2010]. This means that each fold has the same number of examples from
129 each class. We will report results with both balanced and unbalanced data
130 foldings, only to discover, it does not really matter.

131 **Refolding?** The standard practice in neuroimaging is to permute labels
132 and refold the data after each permutation, so that the balance of the classes
133 in each fold is preserved. We will adhere to this practice due to its popularity,
134 even though it can be simplified by permuting features instead of labels, as
135 done by Golland et al. [2005].

136 **How many folds?** Different authors suggest different rules for the number
137 of folds. We will look into the effect of the number of folds.

How to estimate accuracy? Low accuracies, even 0, are evidence that
the classes are separated so that for our purposes, we should consider the
departure from chance level $|\hat{\mathcal{E}}_{\mathcal{A}} - 0.5|$ as candidate test statistic. For un-
balanced classes, chance level is not 0.5, but rather the probability of
the majority class, we denote by $\hat{\pi}$. This suggests the following test statistic
 $|\hat{\mathcal{E}}_{\mathcal{A}} - \hat{\pi}|$. Since we will be aggregating these statistics over random data sets

where $\hat{\pi}$ may vary, it seems appropriate to standardize the scale. We thus study, along with the naive accuracy estimate, $\hat{\mathcal{E}}_{\mathcal{A}}$, also the *z-scored accuracy* of algorithm \mathcal{A} :

$$\hat{\mathcal{Z}}_{\mathcal{A}} := \frac{|\hat{\mathcal{E}}_{\mathcal{A}} - \hat{\pi}|}{\sqrt{\hat{\pi}(1 - \hat{\pi})}}. \quad (5)$$

138 Table 1 collects an initial battery of tests we will be comparing.

Name	Algorithm	Accuracy	Z-scored	Parameters
Hotelling	Hotelling	—	—	—
Hotelling.shrink	Hotelling	—	—	—
sd	SD	—	—	—
lda.CV.1	LDA	V-fold	FALSE	—
lda.CV.2	LDA	V-fold	TRUE	—
lda.noCV.1	LDA	Resubstitution	FALSE	—
lda.noCV.2	LDA	Resubstitution	TRUE	—
svm.CV.1	SVM	V-fold	FALSE	cost=10
svm.CV.2	SVM	V-fold	FALSE	cost=0.1
svm.CV.3	SVM	V-fold	TRUE	cost=10
svm.CV.4	SVM	V-fold	TRUE	cost=0.1
svm.noCV.1	SVM	Resubstitution	FALSE	cost=10
svm.noCV.2	SVM	Resubstitution	FALSE	cost=0.1
svm.noCV.3	SVM	Resubstitution	TRUE	cost=10
svm.noCV.4	SVM	Resubstitution	TRUE	cost=0.1

Table 1: This table collects the various test statistics we will be studying. Three are population tests: *Hotelling*, *Hotelling.shrink*, and *sd*. *Hotelling* is the classical two-group T^2 statistic. *Hotelling.shrink* is a high dimensional version with the regularized covariance from Schäfer and Strimmer [2005]. *sd* is another high dimensional version of the T^2 , from Srivastava et al. [2013]. The rest of the tests are variations of the linear SVM, and Fisher’s LDA, with varying accuracy measures, cross validated or not, and varying tuning parameters. For example, *svm.CV.4* is a linear SVM implemented with the *svm* R function [Meyer et al., 2015], the cost parameter set at 0.1, and using the cross validated z-scored accuracy in Eq. 5. Another example is *lda.noCV.1*, which is Fisher’s LDA, returning the resubstitution accuracy.

139

140 3 Controlling the False Positive Rate

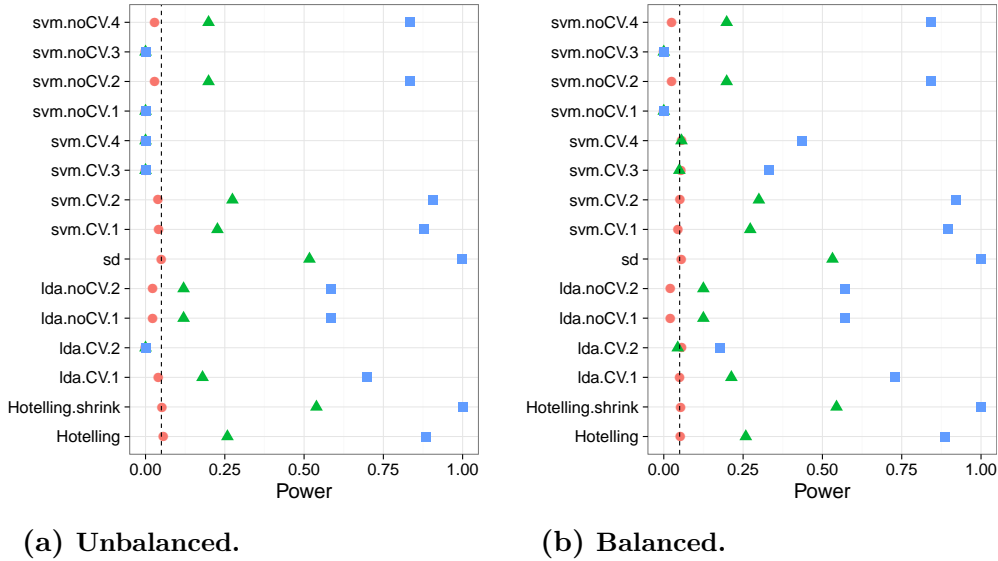
141 Our simulation show that all of the tests considered conserve the desired
142 0.05 false positive rate, up to varying levels of conservatism. This can be

143 seen from the fact that the probability of rejection is no larger than 0.05 in
 144 the absence of any effect, encoded by a red circle. This is true, in particular
 145 if:

- 146 (a) The folds are balanced or not (Figures 1,6 and 7)
- 147 (b) The tuning parameters are varied (cost=10 versus cost=0.1).
- 148 (c) The number of folds is varied (Figures 6 and 7).
- 149 (d) The noise is heavytailed (Figure 8b).
- 150 (e) The problem is high or low dimensional (Figure 9.)
- 151 (f) The noise is correlated (Figure 10b).

152 We also observe that the most conservative tests are the resubstitution ac-
 153 curacy statistics. We return to this matter in the Discussion.

Figure 1: The power of a permutation test with various test statistics. The power on the x axis. Effect are color and shape coded. The various statistics on the y axis. Their details are given in Table 1. Effects vary over 0 (red circle), 0.25 (green triangle), and 0.5 (blue square). Simulation details in Appendix B. Cross-validation was performed with balanced and unbalanced data folding. See sub-captions.



154 4 Power

155 Having established that all of the tests in our battery control the false pos-
 156 itive rate, it remains to be seen if they have similar power– especially when
 157 comparing population tests to accuracy tests. From the simulation results
 158 reported in Appendix C we collect the following insights:

- 159 1. Population tests have more power than accuracy tests in all our con-
160 figurations.
- 161 2. The conservativeness decays as the sample grows (Figures 9a, 9b and
162 10a)
- 163 3. For heavy tailed distributions (Figure 8b), the extra power of the pop-
164 ulation test vanishes.
- 165 4. Regularization is most beneficial to power in low signal to noise (SNR)
166 regimes. Low SNR may be the result of a high-dimensional problem,
167 or due to correlations. Indeed, the presence of positive correlations
168 amplifies the contribution of regularization to power ((Figure 10b)).
- 169 5. The z-scoring of the accuracies was introduced to deal with unbalanced
170 foldings. If the z-scoring has any effect at all, it merely kills power.
- 171 6. Both accuracy and population tests are inappropriate for scale alter-
172 natives (Figure 8a). This was to be expected and is reported mostly as
173 a sanity check.
- 174 7. Balanced folding only affects the z-scored accuracy, in the opposite
175 direction than we anticipated.
- 176 8. Increasing the SVM's cost parameter, which reduces the number of
177 support vectors entering the classifier, reduces power.

178 The major insight from simulations is that the use of accuracy tests for
179 signal detection is underpowered compared to population tests. We have not
180 established, however, that the dominance of the population tests is not due to
181 their regularization. Indeed, the unregularized *Hotelling* test, is only slightly
182 superior to the accuracy tests. We return to this matter in Section 6.5. We
183 now verify our finding on a neuroimaging dataset.

184 5 Neuroimaging Example

185 Figure 2 is an application of both a population and an accuracy test to the
186 data of Pernet et al. [2015]. The authors of Pernet et al. [2015] collected fMRI
187 data while subjects were exposed to the sounds of human speech (vocal), and
188 other non-vocal sounds. Each subject was exposed to 20 sounds of each type,
189 totaling in $n = 40$ trials. The study was rather large and consisted of about

190 200 subjects. The data was kindly made available by the authors at the
 191 OpenfMRI website².

192 We perform group inference using within-subject permutations along the
 193 analysis pipeline of Stelzer et al. [2013], which was also reported in Gilron
 194 et al. [2016]. For completeness, the pipeline is described in Appendix A. To
 195 demonstrate our point, we compare the *sd* population test with the *svm.cv.1*
 196 accuracy test.

197 In agreement with our simulation results, the population test (*sd*) dis-
 198 covers more brain regions of interest when compared to an accuracy test
 199 (*svm.cv.1*). The former discovers 1,232 regions, while the latter only 441, as
 200 depicted in Figure 2. We emphasize that both test statistics were compared
 201 with the same permutation scheme, and the same error controls, so that any
 202 difference in detections is due to their different power.

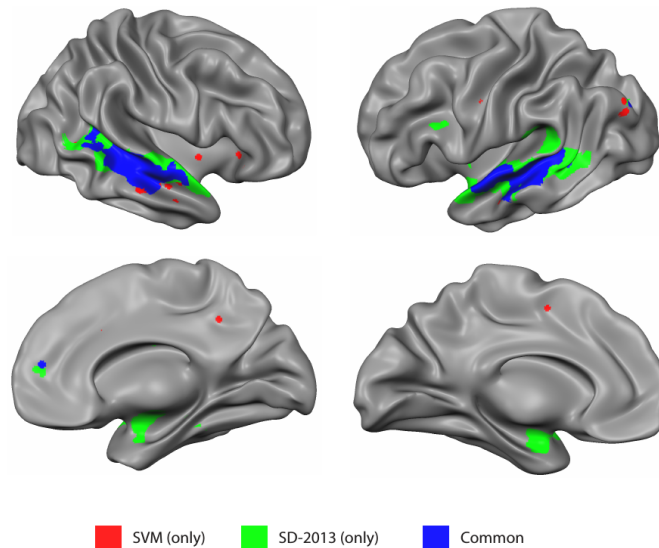


Figure 2: Brain regions encoding information discriminating between vocal and non-vocal stimuli. Map reports the centers of 27-voxel sized spherical regions, as discovered by an accuracy test (*svm.cv.1*), and a population test (*sd*). *svm.cv.1* was computed using 5-fold cross validation, and a cost parameter of 1. Region-wise significance was determined using the permutation scheme of Stelzer et al. [2013], followed by region-wise $FDR \leq 0.05$ control using the Benjamini-Hochberg procedure [Benjamini and Hochberg, 1995]. Number of permutations equals 400. The population test detect 1,232 regions, and the accuracy test 441, 399 of which are common to both. For the details of the analysis see Appendix A and Gilron et al. [2016].

²<https://openfmri.org/>

203 6 Discussion

204 We have set out to understand which of the tests is more powerful: the ac-
205 curacy test or the population test. No amount of simulations can replace the
206 insight provided by a closed-form analytic result. The finite sample power
207 of permutation tests is a formidable mathematical problem, so we currently
208 content ourselves with simulations. We have concluded that the population
209 tests are typically preferable. Their high dimensional versions, such as Sri-
210 vastava [2007] and Schäfer and Strimmer [2005], are particularly well suited
211 for neuroimaging problems such as MVPA. We attribute this to several ef-
212 fects:

- 213 (a) The discrete nature of the accuracy test in finite samples.
- 214 (b) Inefficient use of the data when validating with a holdout set.
- 215 (c) The lack of regularization in high SNR regimes (high dimension or cor-
216 relations).

217
218 The degree of discretization is governed by the sample size. For this
219 reason, an asymptotic analysis such as Ramdas et al. [2016] may uncover
220 the holdout inefficiency, but will not uncover the discretization effect. An
221 asymptotic analysis of a finite complexity model would also fail to reveal the
222 effect of the concentration of the resubstitution accuracy near 1. This effect
223 would render the resubstitution estimates a legitimate asymptotic test, and
224 a terrible finite sample test.

225 The presence of heavy tails shrinks the power advantage of the population
226 tests over accuracy tests. Our empirical example suggests that even if the
227 population test does not necessarily dominate the accuracy test in power,
228 empirically, it does have an advantage.

229 The practical advice for the practitioner, is that for the purpose of signal
230 detection, there is typically a population test that is more powerful than an
231 accuracy test. The class of population tests we examined, in particular their
232 regularized versions, are good performers in a wide range of simulation setups
233 and empirically. They are also typically easier to implement, and faster to
234 run, since no cross validation will be involved.

235 6.1 Ease of implementation

236 A very important consideration is the ease of implementation. The need
237 for cross validation of the accuracy test greatly increases its computational
238 complexity. Moreover, programming with discrete statistics is more prone to
239 errors. This is because their unforgiveness to the type of inequalities used.
240 Indeed, mistakenly replacing a weak inequality with a strong inequality in

one’s program may considerably change the results. This is not the case for continuous test statistics.

6.2 Reservations

Some reservations to the generality of our findings are in order. Firstly, not all accuracy tests are concerned with signal detection. Consider brain decoding for machine interfaces, or clinical diagnosis, where the presence of a medical condition is predicted from imaging data [e.g. Olivetti et al., 2012, Wager et al., 2013]. In those examples, the purpose of the test is not to detect a difference between classes, but to actually test the performance of a particular classifier.

Secondly, it may be argued that accuracy tests permits the separation between classes in high dimensions, such as in *reproducing kernel Hilbert spaces* (RKHS) by using non-linear predictors while population tests do not. This is a false argument—accuracy test do not have any more flexibility than population tests. Indeed, it is possible to test for location in the same space the classifier is learned. Gretton et al. [2012] is an example where the test for location is performed in RKHS. It is also possible to test for the equality of two multivariate distributions on an arbitrary, unspecified manifold [e.g. Heller et al., 2013][TODO: verify]. On the other hand, based on our experience, and the reported neuroimaging example, we find that a population test in the original feature space is a simple and powerful approach to signal detection.

6.3 A good accuracy test

For the cases a population test cannot replace an accuracy test, we collect some conclusions and best practices from our simulations. We give particular emphasis in this section to V-fold cross validation due to its popularity, but note that sampling the test set with replacement is actually preferable, as we discuss in Section 6.4.

Sample size. The conservativeness of accuracy tests decrease with sample size.

Permute features. Permuting features, such as in Golland et al. [2005], is easier than permuting labels. It allows to preserve the balance of folds after a permutation, without refolding.

274 **Resubstitution accuracy in low dimension.** Resubstitution accuracy
 275 is useful in low SNR regimes, such as low dimensional problems, because it
 276 avoids cross validation without compromising power. In high dimension, the
 277 power loss is considerable compared to a cross validated approach. We at-
 278 tribute this to the compounding of discretization and concentration effects:
 279 the difference between the sampling distribution of the resubstitution accu-
 280 racy is simply indistinguishable under the null and under the alternative.
 281 In low dimensional problems, the discretization is less impactful, and the
 282 computational burden of cross validation can be avoided by using the resub-
 283 stitution accuracy. There is a fundamental difference between V-folding and
 284 resubstitution. The latter should not be thought of as the limit of the former.

285 **Regularize** Regularizing a classifier proves crucial to detection power in
 286 low SNR regimes; in high dimension in particular. We also conjecture that
 287 the power-maximizing regularization is larger than the error-minimizing reg-
 288 ularization.

289 **Don't z-score.** There is no gain in z-scoring the accuracy scores. Our
 290 motivating rational was clearly flawed. [TODO: why?]

291 6.4 Smoothing accuracy estimates

292 It may be possible to alleviate the effect of discretization by appropriate
 293 cross-validation. The discreteness of the accuracy statistic is governed by the
 294 number of examples in the union of test sets, over all validation iterations.
 295 For V-fold CV, for instance, the accuracy may assume as many values as the
 296 sample size. This suggests that the accuracy can be “smoothed” by allowing
 297 the test sample to be drawn with replacement. An algorithm that samples
 298 test sets with replacement is the *leave-one-out bootstrap estimator*, and its
 299 derivatives, such as the *0.632 bootstrap*, and *0.632+ bootstrap* [Hastie et al.,
 300 2003, Sec 7.11].

Definition 3 (bLOO). The *leave-one-out bootstrap* estimate is the average accuracy of the holdout observations, over all bootstrap samples. Denoting by \mathcal{S}^b , a bootstrap sample b , sampled with replacement from \mathcal{S} . Also denote by $C^{(i)}$ the index set of bootstrap samples, b , not containing observation i . The leave-one-out bootstrap estimate, $\hat{\mathcal{E}}_A^{bLOO}$, is defined as:

$$\hat{\mathcal{E}}_A^{bLOO} := \frac{1}{n} \sum_{i=1}^n \frac{1}{|C^{(i)}|} \sum_{b \in C^{(i)}} \mathcal{I}\{\mathcal{A}_{\mathcal{S}^b}(x_i) = y_i\}. \quad (6)$$

where $|A|$ is the cardinality of set A . Equivalently [TODO: verify], denoting by $S^{(b)}$ the indexes of observations, i , that are *not* in the bootstrap sample b and are not empty,

$$\hat{\mathcal{E}}_{\mathcal{A}}^{bLOO} = \frac{1}{B} \sum_{b=1}^B \frac{1}{|S^{(b)}|} \sum_{i \in S^{(b)}} \mathcal{I}\{\mathcal{A}_{S^b}(x_i) = y_i\}. \quad (7)$$

Definition 4 (b0.632). The *0.632 bootstrap* estimator, $\hat{\mathcal{E}}_{\mathcal{A}}^{0.632}$, is defined as

$$\hat{\mathcal{E}}_{\mathcal{A}}^{0.632} := 0.368 \hat{\mathcal{E}}_{\mathcal{A}}^{Resub} + 0.632 \hat{\mathcal{E}}_{\mathcal{A}}^{bLOO}. \quad (8)$$

Simulation results reported in Figure 3 with naming conventions in Table 2. It can be seen that selecting test sets with replacement does increase the power, when compared to V-fold cross validation, but still falls short from the power of population tests. It can also be seen that power increases with the number of bootstrap replications, as was to be expected, since more replications reduce the level of discretization. The type of bootstrap, bLOO versus b0.632, does not change the power.

Name	Algorithm	Accuracy	B	Z-scored	Parameters
lda.Boot.1	LDA	b0.632	10	FALSE	–
lda.Boot.2	LDA	bLOO	10	FALSE	–
svm.Boot.1	SVM	b0.632	10	FALSE	cost=1e1
svm.Boot.2	SVM	bLOO	10	FALSE	cost=1e1
svm.Boot.3	SVM	b0.632	50	FALSE	cost=1e1
svm.Boot.4	SVM	bLOO	50	FALSE	cost=1e1

Table 2: The same as Table 1 for bootstrapped accuracy estimates. bLOO and b0.632 are defined in definitions 3 and 4 respectively. B denotes the number of Bootstrap samples.

6.5 High dimensional classifiers

Inspecting Figure 1a (for instance), it can be seen that Hotelling’s T^2 test has similar power as accuracy tests. It should thus be argued that the real advantage of the population tests is due to their adaptation to high dimension by regularization, and not only to discretization. To study this, we call upon several *regularized classifiers*, designed for high dimensional problems. In the spirit of the regularized covariance of *Hotelling.shrink*, we try an l_2



Figure 3: Bootstrap— The power of a permutation test with various test statistics. The power on the x axis. Effect are color and shape coded. The various statistics on the y axis. Their details are given in tables 1 and 2. Effects vary over 0 (red circle), 0.25 (green triangle), and 0.5 (blue square). Simulation details in Appendix B.

regularized SVM Friedman et al. [2010], and shrinkage based LDA [Pang et al., 2009, Ramey et al., 2016]. In the spirit of the diagonalized covariance of *sd*, we try a diagonalized LDA [Dudoit et al., 2002], a.k.a. *Gaussian naive Bayes*.

Simulation results reported in Figure 4 with naming conventions in Table 3. It can be seen that regularizing a classifier in high dimension, just like a parameter test, improves power. It can also be seen that (regularized) parameter tests are still more powerful than (regularized) accuracy tests. This was to be expected, since we already saw in (e.g. Figure 1a) that the unregularized parameter test, *Hotelling*, is slightly more powerful than the regularized accuracy test, *svm.CV.1* for instance.

We can compound regularization in this section with the bootstrapping from Section 6.4, to improve finite sample power of the accuracy tests. This is done in the *svm.highdim.2* test, which still falls short from the power of the population tests, but is a much more powerful accuracy test than the original non-regularized, V-fold validated, version of *svm.CV.1*.

Name	Algorithm	Accuracy	Z-scored	Parameters
svm.highdim.1	SVM	V-fold	FALSE	cost=1e-1, V=4
svm.highdim.2	SVM	b0.632	FALSE	cost=1e-1, B=50
lda.highdim.1	LDA	V-fold	FALSE	V=4
lda.highdim.2	LDA	V-fold	FALSE	V=4
lda.highdim.3	LDA	V-fold	FALSE	V=4

Table 3: The same as Table 1 for regularized (high dimensional) predictors. *svm.highdim.1* is an l_2 regularized SVM Friedman et al. [2010]. *svm.highdim.2* is the same with b0.632 instead of V-fold cross validation. *lda.highdim.1* is the Diagonal Linear Discriminant Analysis of Dudoit et al. [2002]. *lda.highdim.2* is the High-Dimensional Regularized Discriminant Analysis of Ramey et al. [2016]. *lda.highdim.3* is the Shrinkage-based Diagonal Linear Discriminant Analysis of Pang et al. [2009].

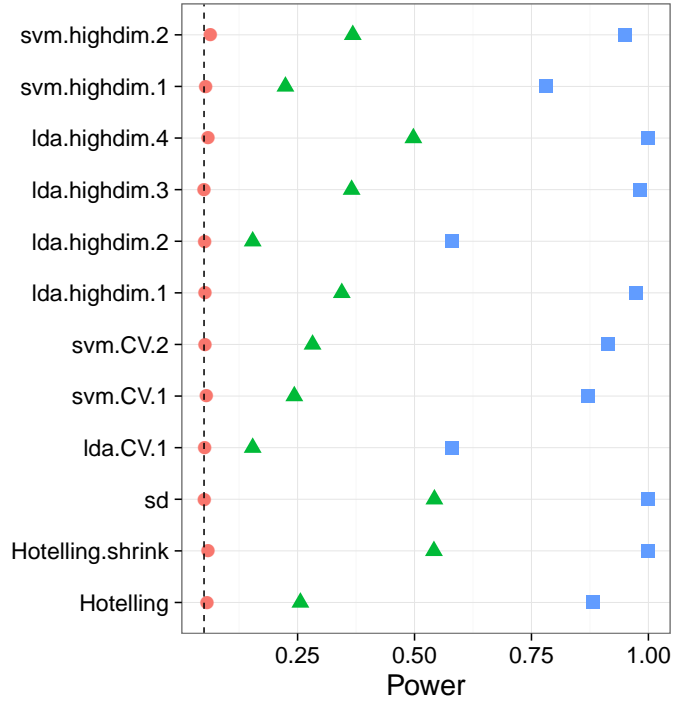


Figure 4: **HighDim Classifier**— The power of a permutation test with various test statistics. The power on the x axis. Effect are color and shape coded. The various statistics on the y axis. Their details are given in tables 1 and 3. Effects vary over 0 (red circle), 0.25 (green triangle), and 0.5 (blue square). Simulation details in Appendix B.

333 6.6 Related Literature

334 Ojala and Garriga [2010] study the power of two accuracy tests: one test-
 335 ing the “no signal” null hypothesis, and the other testing the “independent
 336 features” null hypothesis. They perform an asymptotic analysis, and a sim-
 337 ulation study. They also apply various classifiers to various data sets. Their
 338 emphasis is the effect of the underlying classifier on the power, and the po-
 339 tential of the “independent features” test for feature selection. This is a very
 340 different emphasis from our own.

341 Olivetti et al. [2012] and Olivetti et al. [2014] looked into the problem of
 342 choosing a good accuracy test. They propose a new test they call an *indepen-*
 343 *dence test*, and demonstrate by simulation that it has more power than other
 344 accuracy tests, and can deal with non-balanced data sets. We did not include
 345 this test in the battery we compared, but we note the following: (a) The in-
 346 dependence test of Olivetti et al. [2012] relies on a discrete test statistic. It
 347 may thus be improved with the methods discussed in this section, before the
 348 application of Olivetti et al. [2012]’s independence test. (b) In contrast with
 349 the underlying motivation of Olivetti et al. [2012]’s independence test, we
 350 did not find that balancing the data folds is crucial for an accuracy test.

351 Golland et al. [2005] study accuracy tests using simulation, neuroimaging
 352 data, genetic data, and analytically. Their analytic results formalize our in-
 353 tuition from Section 1 on the effect of concentration of the accuracy statistic:
 354 The finite Vapnik–Chervonenkis (VC) dimension requirement [Golland and
 355 Fischl, 2003, Sec 4.3] prevents the permutation p-value from (asymptotically)
 356 concentrating near 1. Like ourselves, they also find that the power increases
 357 with the size of the test set (Figure 4, middle). This is seen in their Figure 4,
 358 where the size of the test-set, K , governs the discretization. Since they per-
 359 mutate features, not labels, then all their permutation samples are balanced,
 360 and there is no issue of refolding.

361 Golland et al. [2005] simulate the power of accuracy tests by sampling
 362 from a Gaussian mixture family of models, and not from a location family
 363 as our own simulations. Under their model $(x_i|y_i = 1) \sim p\mathcal{N}(\mu_1, I) +$
 364 $(1 - p)\mathcal{N}(\mu_2, I)$ and $(x_i|y_i = -1) \sim (1 - p)\mathcal{N}(\mu_1, I) + p\mathcal{N}(\mu_2, I)$. Varying p
 365 interpolates between the null distribution ($p = 0.5$) and a location shift model
 366 ($p = 0$). We now perform the same simulation as Golland et al. [2005], after
 367 parameterizing p so that $p = 0$ corresponds to the null model, and in the
 368 same dimensionality as our previous simulations We find that also in this
 369 mixture class of models a population test has more power than an accuracy
 370 test (Figure 5).

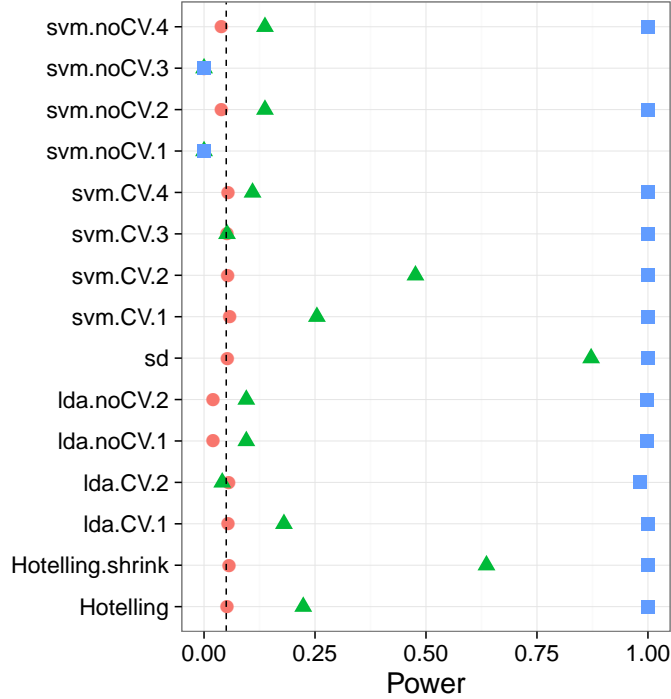


Figure 5: **Mixture**— $\mathbf{x}_i = \chi_i \mu + \eta_i$; $\chi_i = \{-1, 1\}$ and $Prob(\chi_i = 1) = (1/2 - p)^{y_i^*} (1/2 + p)^{1-y_i^*}$. μ is a p -vector with $3/\sqrt{p}$ in all coordinates. The effect, p , is color and shape coded and varies over 0 (red circle), $1/4$ (green triangle) and $1/2$ (blue square).

6.7 Epilogue

Given all the above, we find the popularity of accuracy tests quite puzzling. We believe this is due to a reversal of the inference cascade. Researchers first fit a classifier, and then ask if the classes are any different. Were they to start by asking if classes are any different, and only then try to classify, then population tests would naturally arise as the preferred method. As put by Ramdas et al. [2016]:

The recent popularity of machine learning has resulted in the extensive teaching and use of prediction in theoretical and applied communities and the relative lack of awareness or popularity of the topic of Neyman-Pearson style hypothesis testing in the computer science and related “data science” communities.

And more simply by Frank Harrell in the CrossValidated Q&A site³:

³<http://stats.stackexchange.com/questions/17408/how-to-assess-statistical-significance-of-the-accuracy-of-a-classifier>.

384 ... your use of proportion classified correctly as your accuracy
385 score. This is a discontinuous improper scoring rule that can be
386 easily manipulated because it is arbitrary and insensitive.

387 **7 Acknowledgments**

References

- T. W. Anderson. *An Introduction to Multivariate Statistical Analysis*. Wiley-Interscience, Hoboken, NJ, 3 edition edition, July 2003. ISBN 978-0-471-36091-9.
- Y. Benjamini and Y. Hochberg. Controlling the false discovery rate: a practical and powerful approach to multiple testing. *JOURNAL-ROYAL STATISTICAL SOCIETY SERIES B*, 57:289–289, 1995.
- S. Dudoit, J. Fridlyand, and T. P. Speed. Comparison of Discrimination Methods for the Classification of Tumors Using Gene Expression Data. *Journal of the American Statistical Association*, 97(457):77–87, Mar. 2002. ISSN 0162-1459. doi: 10.1198/016214502753479248.
- J. Friedman, T. Hastie, and R. Tibshirani. Regularization Paths for Generalized Linear Models via Coordinate Descent. *Journal of Statistical Software*, 33(1):1–22, 2010.
- R. Gilron, J. Rosenblatt, O. Koyejo, R. A. Poldrack, and R. Mukamel. Quantifying spatial pattern similarity in multivariate analysis using functional anisotropy. *arXiv:1605.03482 [q-bio]*, May 2016.
- P. Golland and B. Fischl. Permutation tests for classification: towards statistical significance in image-based studies. In *IPMI*, volume 3, pages 330–341. Springer, 2003.
- P. Golland, F. Liang, S. Mukherjee, and D. Panchenko. Permutation Tests for Classification. In P. Auer and R. Meir, editors, *Learning Theory*, number 3559 in Lecture Notes in Computer Science, pages 501–515. Springer Berlin Heidelberg, June 2005. ISBN 978-3-540-26556-6 978-3-540-31892-7. doi: 10.1007/11503415_34.
- T. R. Golub, D. K. Slonim, P. Tamayo, C. Huard, M. Gaasenbeek, J. P. Mesirov, H. Coller, M. L. Loh, J. R. Downing, M. A. Caligiuri, C. D. Bloomfield, and E. S. Lander. Molecular Classification of Cancer: Class Discovery and Class Prediction by Gene Expression Monitoring. *Science*, 286(5439):531–537, Oct. 1999. ISSN 0036-8075, 1095-9203. doi: 10.1126/science.286.5439.531.
- A. Gretton, K. M. Borgwardt, M. J. Rasch, B. Schölkopf, and A. Smola. A Kernel Two-sample Test. *J. Mach. Learn. Res.*, 13:723–773, Mar. 2012. ISSN 1532-4435.

- 422 T. Hastie, R. Tibshirani, and J. Friedman. *The Elements of Statistical Learn-*
423 *ing*. Springer, July 2003. ISBN 0-387-95284-5.
- 424 R. Heller, Y. Heller, and M. Gorfine. A consistent multivariate test of associ-
425 ation based on ranks of distances. *Biometrika*, 100(2):503–510, Jan. 2013.
426 ISSN 0006-3444, 1464-3510. doi: 10.1093/biomet/ass070.
- 427 J. Hemerik and J. Goeman. Exact testing with random permutations.
428 *arXiv:1411.7565 [math, stat]*, Nov. 2014.
- 429 H. Hotelling. The Generalization of Student’s Ratio. *The Annals of Math-*
430 *ematical Statistics*, 2(3):360–378, Aug. 1931. ISSN 0003-4851, 2168-8990.
431 doi: 10.1214/aoms/1177732979.
- 432 W. Jiang, S. Varma, and R. Simon. Calculating confidence intervals for
433 prediction error in microarray classification using resampling. *Statistical*
434 *Applications in Genetics and Molecular Biology*, 7(1), 2008.
- 435 L. Juan and H. Iba. Prediction of tumor outcome based on gene expression
436 data. *Wuhan University Journal of Natural Sciences*, 9(2):177–182, Mar.
437 2004. ISSN 1007-1202, 1993-4998. doi: 10.1007/BF02830598.
- 438 N. Kriegeskorte, R. Goebel, and P. Bandettini. Information-based functional
439 brain mapping. *Proceedings of the National Academy of Sciences of the*
440 *United States of America*, 103(10):3863–3868, July 2006. ISSN 0027-8424,
441 1091-6490. doi: 10.1073/pnas.0600244103.
- 442 E. L. Lehmann. Parametric versus nonparametrics: two alternative method-
443 ologies. *Journal of Nonparametric Statistics*, 21(4):397–405, 2009. ISSN
444 1048-5252. doi: 10.1080/10485250902842727.
- 445 G. J. McLachlan. The bias of the apparent error rate in discriminant analysis.
446 *Biometrika*, 63(2):239–244, Jan. 1976. ISSN 0006-3444, 1464-3510. doi:
447 10.1093/biomet/63.2.239.
- 448 D. Meyer, E. Dimitriadou, K. Hornik, A. Weingessel, and F. Leisch. *e1071:*
449 *Misc Functions of the Department of Statistics, Probability Theory Group*
450 *(Formerly: E1071), TU Wien*. 2015. R package version 1.6-7.
- 451 S. Mukherjee, P. Tamayo, S. Rogers, R. Rifkin, A. Engle, C. Campbell,
452 T. R. Golub, and J. P. Mesirov. Estimating dataset size requirements
453 for classifying DNA microarray data. *Journal of Computational Biology:*
454 *A Journal of Computational Molecular Cell Biology*, 10(2):119–142, 2003.
455 ISSN 1066-5277. doi: 10.1089/106652703321825928.

- 456 M. Ojala and G. C. Garriga. Permutation Tests for Studying Classifier Perfor-
457 mance. *Journal of Machine Learning Research*, 11(Jun):1833–1863, 2010.
458 ISSN ISSN 1533-7928.
- 459 E. Olivetti, S. Greiner, and P. Avesani. Induction in Neuroscience with
460 Classification: Issues and Solutions. In G. Langs, I. Rish, M. Grosse-
461 Wentrup, and B. Murphy, editors, *Machine Learning and Interpretation*
462 *in Neuroimaging*, number 7263 in Lecture Notes in Computer Science,
463 pages 42–50. Springer Berlin Heidelberg, 2012. ISBN 978-3-642-34712-2
464 978-3-642-34713-9. doi: 10.1007/978-3-642-34713-9_6.
- 465 E. Olivetti, S. Greiner, and P. Avesani. Statistical independence for the
466 evaluation of classifier-based diagnosis. *Brain Informatics*, 2(1):13–19, Dec.
467 2014. ISSN 2198-4018, 2198-4026. doi: 10.1007/s40708-014-0007-6.
- 468 H. Pang, T. Tong, and H. Zhao. Shrinkage-based Diagonal Discriminant
469 Analysis and Its Applications in High-Dimensional Data. *Biometrics*, 65
470 (4):1021–1029, Dec. 2009. ISSN 1541-0420. doi: 10.1111/j.1541-0420.2009.
471 01200.x.
- 472 F. Pereira, T. Mitchell, and M. Botvinick. Machine learning classifiers and
473 fMRI: A tutorial overview. *NeuroImage*, 45(1, Supplement 1):S199–S209,
474 Mar. 2009. ISSN 1053-8119. doi: 10.1016/j.neuroimage.2008.11.007.
- 475 C. R. Pernet, P. McAleer, M. Latinus, K. J. Gorgolewski, I. Charest, P. E. G.
476 Bestelmeyer, R. H. Watson, D. Fleming, F. Crabbe, M. Valdes-Sosa, and
477 P. Belin. The human voice areas: Spatial organization and inter-individual
478 variability in temporal and extra-temporal cortices. *NeuroImage*, 119:164–
479 174, Oct. 2015. ISSN 1053-8119. doi: 10.1016/j.neuroimage.2015.06.050.
- 480 M. D. Radmacher, L. M. McShane, and R. Simon. A Paradigm for
481 Class Prediction Using Gene Expression Profiles. *Journal of Computa-*
482 *tional Biology*, 9(3):505–511, June 2002. ISSN 1066-5277. doi: 10.1089/
483 106652702760138592.
- 484 A. Ramdas, A. Singh, and L. Wasserman. Classification Accuracy as a Proxy
485 for Two Sample Testing. *arXiv:1602.02210 [cs, math, stat]*, Feb. 2016.
- 486 J. A. Ramey, C. K. Stein, P. D. Young, and D. M. Young. High-Dimensional
487 Regularized Discriminant Analysis. *arXiv preprint arXiv:1602.01182*,
488 2016.
- 489 J. Schäfer and K. Strimmer. A Shrinkage Approach to Large-Scale Covariance
490 Matrix Estimation and Implications for Functional Genomics. *Statistical*

- 491 *Applications in Genetics and Molecular Biology*, 4(1), Jan. 2005. ISSN
492 1544-6115. doi: 10.2202/1544-6115.1175.
- 493 D. K. Slonim, P. Tamayo, J. P. Mesirov, T. R. Golub, and E. S. Lander. Class
494 Prediction and Discovery Using Gene Expression Data. In *Proceedings of*
495 *the Fourth Annual International Conference on Computational Molecular*
496 *Biology*, RECOMB '00, pages 263–272, New York, NY, USA, 2000. ACM.
497 ISBN 978-1-58113-186-4. doi: 10.1145/332306.332564.
- 498 M. S. Srivastava. Multivariate Theory for Analyzing High Dimensional Data.
499 *Journal of the Japan Statistical Society*, 37(1):53–86, 2007. doi: 10.14490/
500 jjss.37.53.
- 501 M. S. Srivastava, S. Katayama, and Y. Kano. A two sample test in high
502 dimensional data. *Journal of Multivariate Analysis*, 114:349–358, Feb.
503 2013. ISSN 0047-259X. doi: 10.1016/j.jmva.2012.08.014.
- 504 J. Stelzer, Y. Chen, and R. Turner. Statistical inference and multiple test-
505 ing correction in classification-based multi-voxel pattern analysis (MVPA):
506 Random permutations and cluster size control. *NeuroImage*, 65:69–82, Jan.
507 2013. ISSN 1053-8119. doi: 10.1016/j.neuroimage.2012.09.063.
- 508 A. W. van der Vaart. *Asymptotic Statistics*. Cambridge University Press,
509 Cambridge, UK ; New York, NY, USA, Oct. 1998. ISBN 978-0-521-49603-
510 2.
- 511 G. Varoquaux, P. R. Raamana, D. Engemann, A. Hoyos-Idrobo, Y. Schwartz,
512 and B. Thirion. Assessing and tuning brain decoders: cross-validation,
513 caveats, and guidelines. working paper or preprint, June 2016.
- 514 T. D. Wager, L. Y. Atlas, M. A. Lindquist, M. Roy, C.-W. Woo, and E. Kross.
515 An fMRI-Based Neurologic Signature of Physical Pain. *New England Jour-*
516 *nal of Medicine*, 368(15):1388–1397, Apr. 2013. ISSN 0028-4793. doi:
517 10.1056/NEJMoa1204471.

518 A Analysis pipeline

519 Here is the analysis pipeline of Stelzer et al. [2013] we for the auditory data in
 520 Gilron et al. [2016]. Denoting by $i = 1, \dots, I$ the subject index, $v = 1, \dots, V$
 521 the voxel index, and $s = 1, \dots, S$ the permutation index. Since regions⁴ are
 522 centered around a unique voxel, the voxel index v also serves as a unique
 523 region index. Algorithm 1 computes a region-wise test statistic, which is
 524 compared to its permutation null distribution computed by Algorithm 2.

Algorithm 1: Compute a group parametric map.

Data: fMRI scans, and experimental design.
Result: Brain map of group statistics: $\{\bar{T}_v\}_{v=1}^V$

```

1 for  $v \in 1, \dots, V$  do
2   for  $i \in 1, \dots, I$  do
3      $T_{i,v} \leftarrow$  test statistic for subject  $i$  in a region centered at  $v$ .
4    $\bar{T}_v \leftarrow \frac{1}{I} \sum_{i=1}^I T_{i,v}$ .
```

Algorithm 2: Compute a permutation p-value map.

Data: fMRI scans of 20 subjects, experimental design.
Result: Brain map of permutation p-values: $\{p_v\}_{v=1}^V$

```

1 for  $s \in 1, \dots, S$  do
2   permute labels;
3    $\bar{T}_v^s \leftarrow$  parametric map
```

⁴*searchlight* or *sphere* in the MVPA parlance

527 B Simulation Details

528 The following details are common to all the reported simulations, unless
529 stated otherwise in a figure’s caption. The R code for the simulations can be
530 found in [TODO].

531 Each simulation is based on 4,000 replications. In each replication, we
532 generate n i.i.d. samples from a shift model $\mathbf{x}_i = \mu \mathbf{y}_i^* + \eta_i$. Where $y_i^* = \{0, 1\}$
533 is the class of subject i in dummy coding. Recalling that $y_i = \{-1, 1\}$ is the
534 class in effect coding, then clearly $y_i = 2y_i^* - 1$. The noise is distributed as
535 $\eta_i \sim \mathcal{N}_p(0, \Sigma)$. The sample size $n = 40$. The dimension of the data is $p = 23$.
536 The covariance $\Sigma = I$. Effects, i.e. shifts μ , are equal coordinate p -vectors
537 with coordinates that vary over $\mu \in \{0, 1/4, 1/2\}$.

538 Having generated the data, we compute each of the test statistics in Ta-
539 ble 1. For test statistics that require data folding, we used 8 folds. We then
540 compute a permutation p-value by permuting the class labels, and recomput-
541 ing each test statistic. We perform 400 such permutations. We then reject
542 the $\mu_i = 0$ null hypothesis if the permutation p-value is smaller than 0.05.
543 The reported power is the proportion of replication where the permutation
544 p-value falls below 0.05.

C Simulation Results

Figure 6: Simulation details in Appendix B except the changes in the sub-captions.



Figure 7: Simulation details in Appendix B except the changes in the sub-captions.



Figure 8: Simulation details in Appendix B except the changes in the sub-captions.



Figure 9: Simulation details in Appendix B except the changes in the sub-captions.

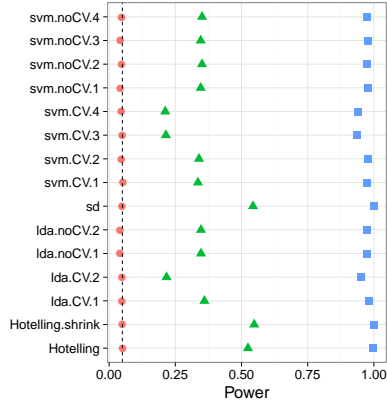


(a) Low-Dimension— False positive rates for $n = 40$.



(b) High-Dimension— False positive rates for $n = 400$.

Figure 10: Simulation details in Appendix B except the changes in the sub-captions.



(a) High-Dimension, local alternative— $n = 400$, $\mu \in \frac{1}{\sqrt{10}} \times \{0, 1/4, 1/2\}$.



(b) AR(1) dependence— $\Sigma_{k,l} = \rho^{|k-l|}$; $\rho = 0.8$.